Soft Matter

Cite this: *Soft Matter*, 2011, **7**, 7291

www.rsc.org/softmatter

PAPER

Refining hydrogelator design: soft materials with improved gelation ability, biocompatibility and matrix for *in situ* synthesis of specific shaped GNP†

Dibyendu Das, Subhabrata Maiti, Sayanti Brahmachari and Prasanta Kumar Das*

Received 6th April 2011, Accepted 23rd May 2011
DOI: 10.1039/c1sm05608e

Despite the continuous surge in the development of new supramolecular gels, the prediction of a gelator's structure still remains elusive. It is also imperative to consolidate the existing inventory of gelators and devise ways to make the gels functional. In the present work, L-phenylalanine based poor (C-16) or non-gelating (C-12 tail) amphiphiles were converted to excellent gelators with the simple incorporation of *N*-terminal protected amino acid/dipeptide at the end of the alkyl tail. More than 6-fold enhancement in gelation efficiency was observed for amino acid/dipeptides incorporated at the tail of amphiphile in comparison to the corresponding unmodified alkyl tail. Interestingly, amphiphile with the tertiary butyloxycarbonyl (Boc) protected amino acid at the tail had better gelation ability than the amphiphile with the aromatic Fmoc (*N*-fluorenyl-9-methoxycarbonyl) protecting group. Spectroscopic investigations (XRD and FTIR) revealed that the modification at the tail compels the amphiphiles to take a different course of self-assembly than that adopted by their predecessors (alkyl tailed gelator, C-16). For example, in the case of the amphiphile having a dipeptide at the tail, formation of β-sheet structure through anti-parallel arrangement between the molecules results in notable improvement in its gelation ability. Most importantly, these tail modified amphiphiles were capable of *in situ* synthesis of gold nanoparticles (GNPs) of specific shape without the help of any external reducing agents in the newly developed soft materials. The biocompatibility of hydrogels is also crucial for their prolific biomedicinal functions. MTT assay showed dramatic improvement in the biocompatibility of the tail modified hydrogelators towards mammalian cells in comparison to the amphiphiles having no amino acid at the tail.

Introduction

Supramolecular gels, a fascinating class of soft materials, are witnessing immense interest in recent times due to their relevance in diversified fields.[1–7] From sensors, actuators in molecular electronics to tissue engineering and biomedicine, the need for versatile soft materials has been felt across disciplines.[8–17] However, it is often observed that when it comes to predicting gelator structures, a serendipitous finding has prevailed over rational designing. In fact foreseeing a gelator design gets even more tentative when we intend to have task specific applications of the soft materials. In this context, in recent years we have been successful in establishing a structural rationale for developing amino acid/dipeptide based amphiphilic gelators, which has excellent ability of immobilizing solvents of extreme nature from water, aromatic hydrocarbons to even ionic liquids.[7,12,18–28] One of the intriguing facets of this structure-gelation property rationale is that when the C-terminal of an aromatic amino acid is attached with a long hydrophobic tail (C-12 to C-16), quaternization at the N-terminal yields hydrogelators. However, except L-tryptophan containing gelators (minimum gelation concentration (MGC) = 0.3%, w/v), the other aromatic amino acids based amphiphiles exhibited conspicuously poor water gelation ability (MGC = 5 and 4%, w/v, for L-phenylalanine and L-tyrosine, respectively).[7,19]

In the quest of improving gelation ability, continuous efforts are mostly emphasized on the design and development of new gelators. At the same time it would be really fascinating to devise ways for upgrading the existing pool of gelators towards augmenting their gelation efficiency with the scope of incorporating functionality to the developed gels. In this regard, exhaustive studies at the polar head (from charge to molecular architecture) of the amphiphilic hydrogelator have been achieved in several previous reports.[7,20,21,24–28] In contrast, variations in the alkyl tail have been primarily restricted to trifling alterations in their chain lengths and thereby to its hydrophobicity.[11,18,21–23] The same

Department of Biological Chemistry, Indian Association for the Cultivation of Science, Jadavpur, Kolkata, 700 032, India. E-mail: bcpkd@iacs.res.in; Fax: +(91)-33-24732805

† Electronic supplementary information (ESI) available: Synthetic scheme for amphiphiles 1–8; temperature dependent CD spectra; TEM images of GNPs synthesized by compound 2 and UV-Vis absorbance spectra of GNPs, ^{1}H NMR spectra and Mass spectra of **1** and **3–8**, ^{13}C NMR spectra of **4–6**. See DOI: 10.1039/c1sm05608e

alkyl tails of these existing amphiphiles can have a more prominent role to play in supramolecular gelation if they are compelled to participate in additional self assembling interactions through judicious functionalization with a supplementary hydrogen bonding moiety.

To this end, the present work reports the development of a new class of amino acid based excellent hydrogelators (Fig. 1) by a simple structural advancement at the tail of non-gelating or poor gelating amphiphile. Incorporation of a tertiary butyloxycarbonyl (Boc) protected amino acid/dipeptides at the alkyl tail

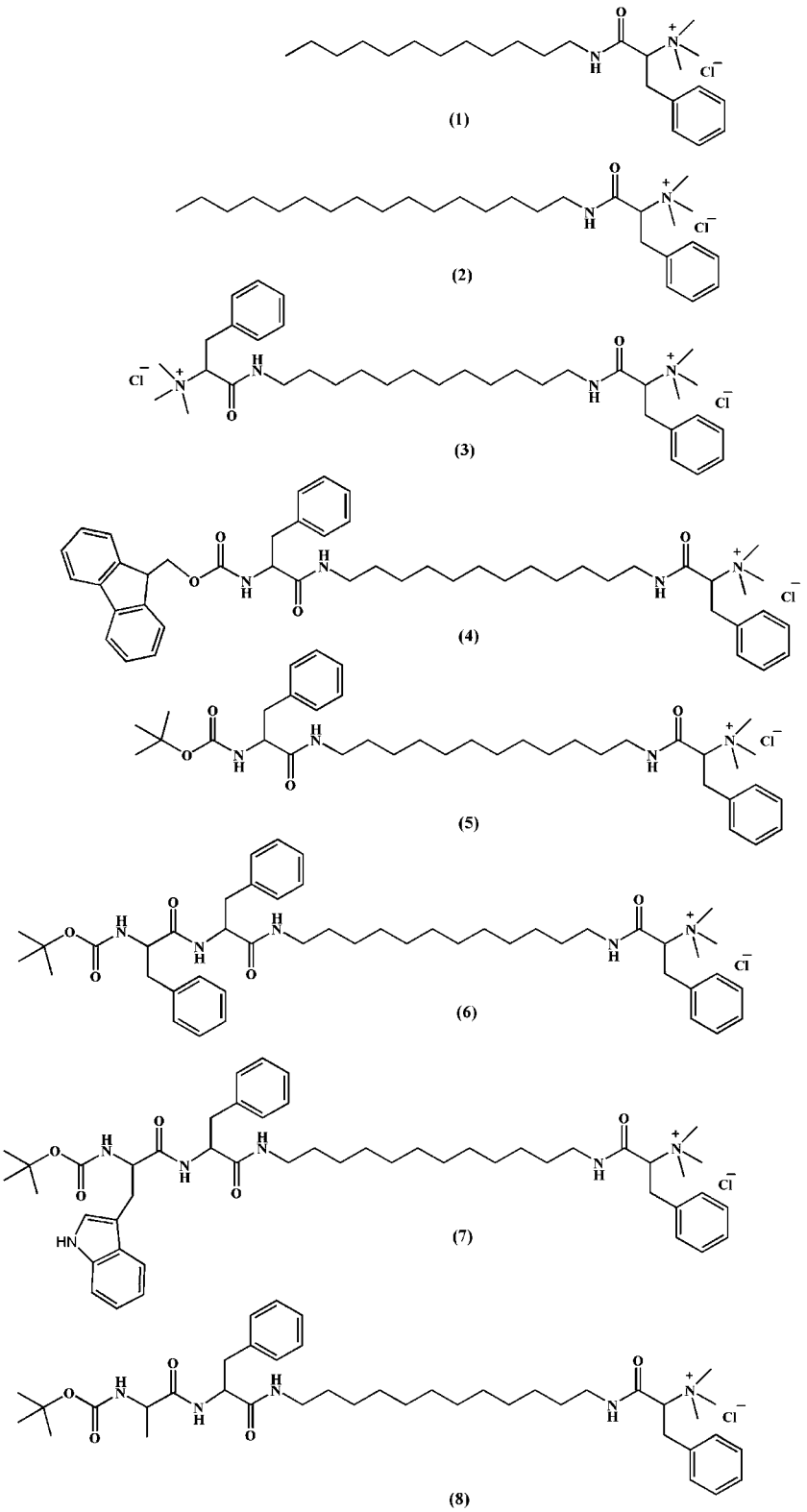

Fig. 1 Structure of **1–8**.

of L-phenylalanine based cationic amphiphile results in a remarkable improvement in gelation ability where a non-gelator (**1** having C-12 tail, Fig. 1) gets converted to an efficient gelator, **5** (MGC = 0.75% w/v, Table 1). In comparison to the C-16 tail length analogue of L-phenylalanine based amphiphile **2** (MGC = 5.0% w/v), more than a 6-fold enhancement in gelation ability was observed for **5**. The amino acid/dipeptide moiety at the tail was varied in order to understand the gelation mechanism and also to establish the structure-gelation property relationships. Insights from XRD and FTIR spectroscopy strongly indicated that the functionalization at the tail promotes a different mode of self assembly which consequently enhanced the gelation ability. The alteration in the supramolecular arrangement of the self-assembled soft materials was used for *in situ* synthesis of gold nanoparticles (GNPs) of different shapes without the help of external reducing agents. Finally, the cell viability of the newly developed hydrogelators was tested to exploit their potentials in diversified biological applications.

Results and discussion

Designing new gelators is a continuous evolution where molecular structure is the key parameter in dictating the self-assembled supramolecular gelation. In this regard, it is important to consolidate knowledge on the structure of existing library of gelator molecules. Judicious analysis on the influence of different segments of these molecules in gelation can bring in the thought of including functionality at the needed domain of the weak/non-gelators to improve its gelation ability. In this context, a library of amphiphilic hydrogelators based on the conventional surfactant architecture featuring a polar head of either cationic or anionic charge with a long hydrophobic tail have been reported in recent years.[18,21–23,27,28] In contrast to the most discussed influence of the polar head, the role of a long alkyl tail in gelation has always been overlooked except in few works possibly because of its typical as well as well-established participation mechanism in self-assembly.[11,18,21–23] At this point, we were curious to investigate whether the influence of this alkyl tail can be made to be dramatic towards improving the supramolecular gelation efficiency of an amphiphile and thereby its applications as functional soft materials.

It is well known from the literature that hydrogen bonding units like amide bond play an instrumental role in the self-assembled gelation.[22,27–30] In this regard, an amino acid has the requisites to provide additional hydrogen bonding interactions, especially when it is attached through an amide bond and also being a natural precursor can possibly augment the biocompatibility of the modified gelators.[29,30] Thus, incorporation of an amino acid as a hydrogen bonding unit at the tail of the amphiphile would be interesting in view of its influence on gelation. However, the proposed alteration should not be done at the cost of losing the critical hydrophobicity of the alkyl tail needed for supramolecular gelation. In fact, it was observed that the gelation ability plummets with the truncation or complete removal of the alkyl tail as the hydrophobic and hydrophilic balance is severely disturbed.[18,23] In order to better understand the proposed effect, we have used an aromatic amino acid L-phenylalanine based cationic amphiphile with a hydrophobic tail of moderate length (twelve carbons, C-12, **1**, Fig. 1). Amphiphile **1** has no gelation ability and was soluble in water which is expected considering the rather poor gelation ability of its longer alkyl tail (C-16) analogues, **2** with MGC of 5.0% w/v (Table 1).[7]

The same structural unit as present in the head group (L-phenylalanine with the quaternized amine) was at first attached as the hydrogen bonding unit at the tail of the amphiphile **1** through an amide linkage (**3**, Fig. 1). However, this L-phenylalanine based di-cationic bolaamphiphile (**3**) did not exhibit any gelation ability in spite of having an additional H-bonding moiety. Rather **3** was found to be soluble in water probably due to the presence of too much hydrophilicity in the amphiphile. The integration of cationic quaternary group on either side of the molecule results in the deviation from optimum hydrophilic-lipophilic balance (HLB) required for hydrogelation. To reduce the hydrophilicity at the tail, the *N*-terminal of L-phenylalanine was protected with the Fmoc (*N*-fluorenyl-9-methoxycarbonyl) group (**4**, Fig. 1) instead of having an additional quaternized amine. This modification would not only decrease the hydrophilic content of the amphiphile, but simultaneously will induce certain degree of hydrophobicity through the planar aromatic moiety, which is very well known to facilitate self-assembled gelation due to the strong π–π interaction between the aromatic rings.[21,29,31,32] Indeed, this alteration induced notable water gelation ability within amphiphile **4** having a MGC of 1.4% w/v at 25 °C (Table 1). Incorporation of additional H-bonding moiety along with aromatic rings at the alkyl tail resulted in the conversion of non-gelator **1** to an efficient hydrogelator **4**.

Considering the observed improvement in gelation ability in the case of **4**, it would be interesting to investigate the influence of the other protecting group of amino acid on the gelation ability of tail modified amphiphilic hydrogelators. For this purpose, instead of the Fmoc moiety, the *N*-terminal of L-phenylalanine was protected with another hydrophobic but non-aromatic Boc group (**5**, Fig. 1). This modification remarkably enhanced the hydrogelation ability further for amphiphile **5** with a MGC of 0.75% w/v (Table 1). Here also the non-gelator **1** gets converted to an excellent hydrogelator **5** due to the inclusion of H-bonding moiety at the alkyl tail with required hydrophobicity. Strikingly, the presence of a non-planar hydrophobic moiety in **5** resulted in a superior gelation than the planar Fmoc containing **4**. Possibly in the case of **5**, the optimum HLB required for efficient hydrogelation had been achieved which is to some extent lost in **4** due to the extended aromaticity of Fmoc moiety. Notably, more than a 6-fold enhancement in gelation efficiency was observed for **5** in comparison to the L-phenylalanine based amphiphilic hydrogelator with C-16 alkyl tail, **2** (MGC = 5.0% w/v, Table 1). In this context, Smith and co-workers have

Table 1 Gelation results of amphiphiles

Amphiphile	State[a]	MGC (%, w/v)
1	S	—
2	TG	5.0
3	S	—
4	TG	1.4
5	TG	0.75
6	TG	2.4
7	S	—
8	TG	1.9

[a] S: solution (soluble up to 8%, w/v); TG: transparent gel.

highlighted the important role of protecting groups of the gelators in modifying the solubility and the saturation point of the system. This concurrently determines the concentration at which network formation takes place leading to gelation.[33]

The observation in the preceding paragraph instigated us to investigate the gelation efficiency of amphiphiles upon introducing a dipeptide moiety at the tail of **1**. To this end, amphiphile **6** was synthesized by attaching a diphenylalanine unit (*N*-terminal protected with Boc) at the tail through an amide bond. Once again the tail modified amphiphile, **6** exhibited improved water gelation ability with MGC = 2.4% w/v. However, in comparison to the amphiphilic gelator **5** having a single L-phenylalanine residue at the tail, the presence of an additional aromatic amino acid (L-phenylalanine) in the dipeptide unit did not augment the gelation efficiency presumably due to the loss in the HLB for amphiphile **6**. The loss in the gelation ability due to the added aromaticity was also observed for amphiphile **7** having a Boc-protected L-tryptophan-L-phenylalanine dipeptide at the terminal end of the long chain. This extended aromaticity of indole moiety in tryptophan even converted a gelator (**6**) to a non-gelator (**7**). This loss of gelation ability could be due to the variation in the hydropathy indices of the amino acids.[12,34] Hydropathy index is the measure of the relative hydrophobic and hydrophilic properties of the side chain residues present in an amino acid. According to this series, hydrophobic amino acids have higher hydropathy indices. Although **6** to **8** have a dipeptide unit at the tail, the HLB of the amino acid present at the terminal end have contrasting hydropathy indices (while L-phenylalanine for **6** and L-alanine for **8** has positive hydropathy number of 2.8 and 1.8, respectively, L-tryptophan for **7** has an index of −0.9). Interestingly, this index implies that although both phenylalanine and tryptophan have aromatic side chain residues, the presence of L-tryptophan in the tail of **7** incorporates substantial degree of hydrophilicity to the amphiphile resulting in water solubility. An extended indole ring containing a hydrophilic-NH group presumably imparts this additional hydrophilicity to L-tryptophan.[33] To avoid this extra aromaticity and hydrophilicity, the additional amino acid in dipeptide moiety was replaced with L-alanine (**8**, the hydropathy index of L-alanine is 1.8). Interestingly, the gelation ability was regained in **8** (MGC = 1.9% w/v, Table 1) by reducing the aromaticity at the hydrophobic domain of the amphiphile. Even, the gelation ability increased in **8** with respect to **6**, but it was found to be lower than **5**. Considering the gelation ability of all the designed amphiphiles (**4–8**), it can be inferred that the presence of an amino acid or peptide (with the protected *N*-terminal) at the tail has a crucial role to induct gelation ability within these molecules. However, the incorporation of one aromatic amino acid with an appropriate protecting group (non-aromatic) at the tail of a non-gelating amphiphile was found to be the befitting alteration for the development of the most efficient hydrogelator, **5**. All the hydrogels were thermoreversible and the gel to sol transition temperature was ~50–60 °C at their MGC.

Characterization of gels

Scanning electron microscopy (SEM). To investigate the supramolecular morphologies formed by the amphiphilic hydrogelators (**4–6**, **8**) in the self assembled state, their dried gels (at MGC) were investigated by field emission scanning electron microscopy (FESEM). Fibrous networks were visible in the microscopic images of all the gels (Fig. 2a–d) and they are different in their nature and sizes. In the case of **4**, the thickness of the fibers was ~100 to 125 nm (Fig. 2a) and the length varied up to micrometers. Interestingly, with the simple alteration in the protection group of the *N*-terminal end (L-phenylalanine) from Fmoc (**4**) to Boc (**5**), a small but significant change in the nature of the fiber was observed (Fig. 2b). Presumably, the molecular structures had an important role in determining the morphology of the networks. In the case of the dried gel of **5** (Fig. 2b), the networks were formed mainly by fibers of diameters ranging from ~200 nm to even ~1 μm, where the thicker fibers are entangled with some very thin fibers. It can also be clearly observed (Fig. 2b) that the intertwined networks were made from the entanglement of thick fibers with pores and thereby providing the capillary forces required entrapment of large number of water molecules (MGC = 0.75% w/v). Furthermore, it was also observed that the fibers of smaller diameters (~100 nm) are coiled together to form thicker fibers of ~1 μm. The lengths of the fibers ranged up to several micrometers with various nodes from where the networks seemed to propagate. Upon incorporation of a diphenylalanine unit (*N*-terminal with Boc protection) at the tail of the amphiphile, the diameter of the fibrils decreased (Fig. 2c).[35] Numerous thin fibrils (~50 nm) were visible in the FESEM images, with some fibrils coiling together to form thicker fibers (~80–100 nm). The xerogel of **8** which had a dipeptide of L-alanine and L-phenylalanine at the tail, also showed intertwined fibrils (Fig. 2d). Furthermore, the thickness of the fibers was found to be little larger (~110 nm) than that observed for **6** with very less population of thinner fibrils. Intriguingly, in comparison to the current set of gelators having a *N*-terminal protected amino acid/dipeptide residue at the terminal end of the alkyl tail, the FESEM image of their predecessor gelator with C-16 alkyl tail, **2** (MGC = 5.0% w/v) had a very less intertwined fibrous morphology.[7] Rather very poorly constructed thick fibers (500–700 nm) were observed for **2**. The lower predominance of the

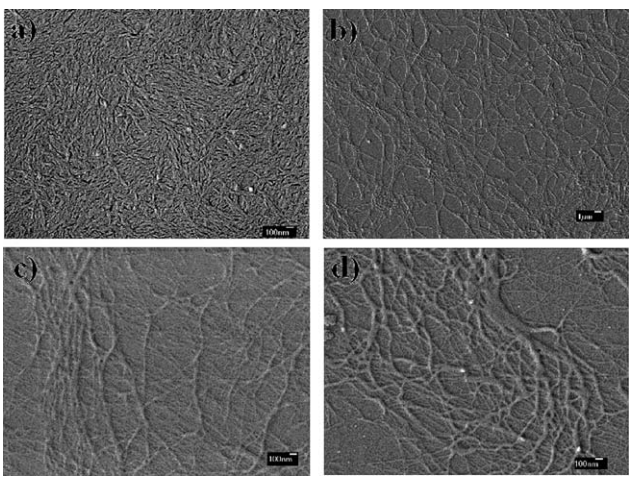

Fig. 2 (a–d) FESEM images of the dried hydrogels of **4**, **5**, **6** and **8** respectively at MGC.

networks with nodes concurrently implies smaller population of pores in **2** resulting in weaker gelation.

Atomic force microscopy (AFM). AFM was also utilized to further investigate the morphology of the gelators **5**, **6** and **8**. Expectedly, fibrous morphology of these amphiphiles was found to be present in the dried gels (Fig. 3). In concurrence with the observed FESEM images, xerogel of the best gelator, **5** showed intertwined fibrous network with the fiber diameter ~150–200 nm (Fig. 3a). However, for **6** the fiber thickness was found to be ~100 nm (Fig. 3b) and also entangled networks were evident in the case of gelator **8** (Fig. 3c). Therefore, the microscopic investigations indicate that the introduction of an amino acid/dipeptide unit at the terminal end of the alkyl tail significantly modifies the supramolecular arrangements of the gelators which concurrently affect the gelation ability.

FTIR. At this point we were intrigued to know how this extra amino acid or dipeptide at the tail of the amphiphile facilitates the supramolecular self-assembled hydrogelation. As this amino acid or peptide moieties are linked through amide bonds, the involvement of hydrogen bonding could be very influential during the self-assembly of new gelators. To probe this, FTIR spectra of **4**, **5** and **6** were taken both at the self-assembled state (in D_2O) and at non self-assembled state (in chloroform, Fig. 4). As a control, the FTIR spectrum of **2** was also taken under similar conditions. Intriguingly, the carbonyl bonds of the new gelators showed a splitting in their amide-I stretching frequency. In the case of **4**, the peaks split in two sub peaks where the peak with large intensity appeared at 1648 cm^{-1} which was associated with a weak peak at 1685 cm^{-1} (Fig. 4a, d). This splitting of the amide peak was not there in the case of **2** (Fig. 4d). Similarly, in the case of **5** and **6**, the peaks were visibly split in to one strong and one weak peak (1650 and 1675 cm^{-1} for **5** and 1639 and 1682 cm^{-1} for **6**, Fig. 4b–d). This splitting of amide peaks is known to be have been observed in the case of β-sheets in proteins and peptides where amide bonds are oriented in anti-parallel mode.[36–38] Furthermore, the difference in the nature of the peaks with respect to the amphiphile having the unmodified alkyl tail (**2**), clearly indicates the involvement of the amide bonds in the formation of antiparallel arrangement during supramolecular gelation of tail modified amphiphiles. Apart from this splitting, the carbonyl stretching frequency (amide-I) which appeared at 1681 cm^{-1} in chloroform for **5** registered blue shift (1650 cm^{-1}) when the spectra was taken at the self assembled state in D_2O (Fig. 4b). Similar shifts in the carbonyl stretching frequency (at amide-I region) were observed for gelator **4** and **6** (Fig. 4a, c). The intermolecular H-bonding between the carbonyl groups of one molecule with the amide-NH of another molecule at the gel state is evident from this shifting.[12,21]

X-ray diffraction (XRD). In order to further establish that the presence of a Boc protected amino acid/dipeptide at the tail of an amphiphilic gelator results in marked alteration in the molecular packing and the possible orientation of the gelator in the supramolecular fibrous networks, we have taken the X-ray diffraction (XRD) spectra of the dried gels of **2**, **5** and **6** (Fig. 5). In case of the weak gelator **2**, the small angle XRD peak (Fig. 5a) corresponds to a *d*-spacing of 3.5 nm, which is smaller than twice the fully extended molecular length of the individual molecule (the length was calculated by the MOPAC AM1 method, CS Chem. Office). Therefore, in the absence of any hydrogen bonding unit at the tail of the amphiphile **2**, the hydrophobic interaction helps in the interdigitation of the long alkyl tails. However, the presence of an amino acid/peptide at the tail of a new set of gelators could hinder the interdigitation between alkyl tails. Indeed, the XRD spectra of the gelators **5** and **6** did not have any small angle peaks which rules out the formation of any interdigitated bilayer structure through the overlapping of alkyl tails (Fig. 5b).[12,21,39] Instead these gelators showed peaks within the 8 to 25° region of 2θ. Interestingly, the xerogel obtained from **5** gave a peak at $2\theta = 19.35°$ which corresponds to a *d*-spacing of 4.58 Å, which matches very well with the distance between the two peptide backbones present in a conventional β-sheet. This peak is accompanied by another peak at $2\theta = 9.63°$ with a *d*-spacing of 9.4 Å (Fig. 5b). These two peaks usually indicate the presence of cross β-structure between the dipeptide moieties with an anti-parallel alignment in the peptide strand.[40–42] The distance of 9.4 Å is the spacing between two laminates. Furthermore the peak at $2\theta = 22.18°$ corresponds to a distance of 4.0 Å which indicates the distance between the two aromatic rings of the amino acid (L-phenylalanine) present at the tail (Fig. 6a). Similarly, in the case of **6**, peaks at $2\theta = 9.85°$ corresponded to a distance of 9.33 Å. The peak at $2\theta = 19.83°$ corresponds to a distance of 4.47 Å which could be the distance between the two molecules comprising of peptide backbone. Here also, a peak at $2\theta = 21.38°$ also indicated the possible aromatic residue stacking separated by 4.15 Å. The spectroscopic evidence gathered from FTIR and XRD helped us to propose a schematic representation of the possible self-assembly *via* an

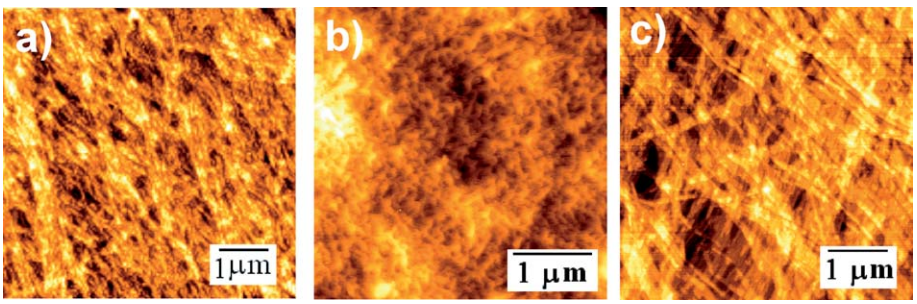

Fig. 3 AFM images of **5**, **6** and **8** at their respective MGC.

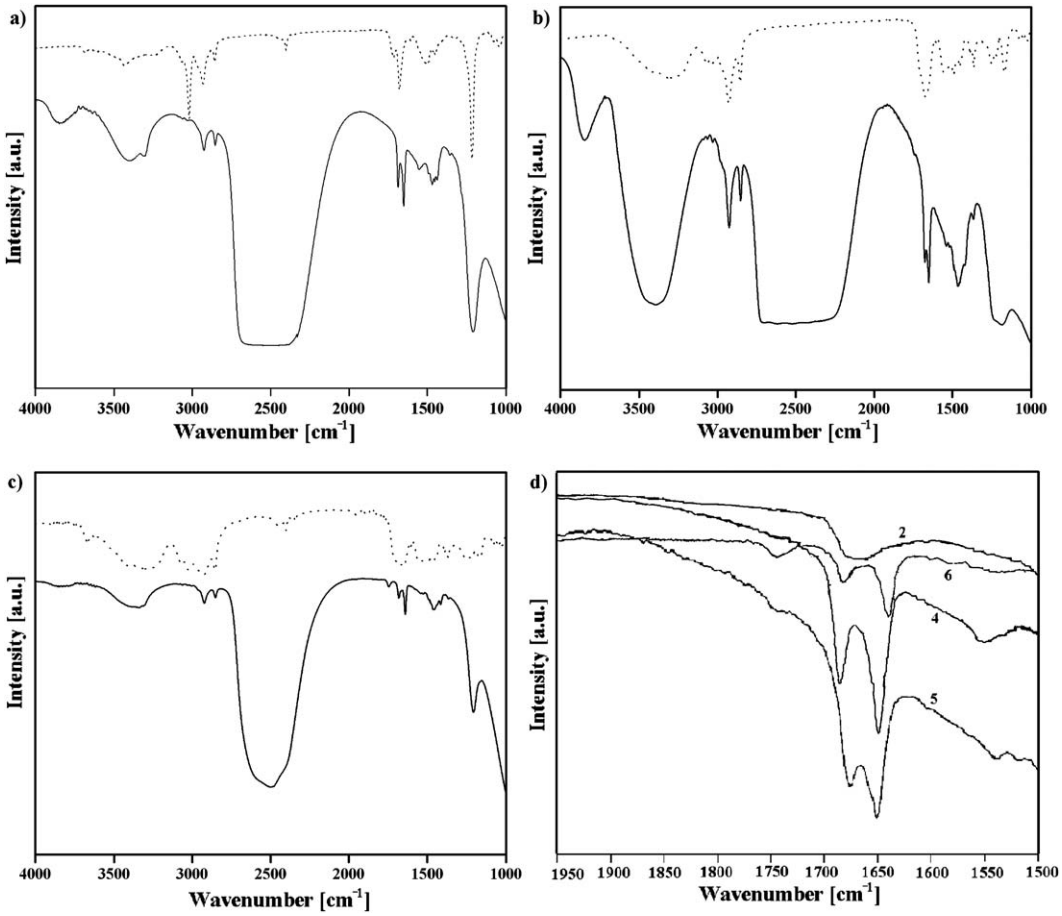

Fig. 4 (a–c) FT-IR spectra of **4–6** in $CHCl_3$ solution (**---**) and in D_2O at gel state (**—**). (d) The strong and weak amide I transmission band of **2** and **4–6**.

antiparallel arrangement of the tail modified gelators (Fig. 6). In the case of **6**, due to the presence of a dipeptide at the tail, the conformation can be termed as cross β-sheet with alternating 10-membered and 14-membered H-bonding (shown in Fig. 6b).

Circular dichroism (CD). The supramolecular arrangement in the self-organized aggregates of the tail modified hydrogelators was also investigated by taking the circular dichroism (CD) spectra of the aqueous solutions of **5** and **6** (Fig. 7). Amphiphile **5** showed positive cotton effect with two maxima in the CD spectra (Fig. 7a) at the amide absorption region, 200-225 nm. This could be attributed to the π–π^* transition of the amide bond along with a shoulder at a longer wavelength from the n–π^* transition of the same.[43–46] Interestingly, in the case of **6**, the presence of one more L-phenylalanine residue (dipeptide) at the tail resulted in negative cotton effects in the CD spectra exhibiting a minima at ~210 nm with a positive peak at 195 nm (Fig. 7b). The spectrum is characteristic of the β-sheet structure of a protein (Fig. 7b).[47–49] However, no such specific CD signature peak was observed for **5**. Despite the amide bonds probably being arranged in an anti-parallel fashion (in accordance with FTIR and XRD spectra), the presence of only one amino acid at the tail of the amphiphile **5**, rules out the possibility of a conventional β-sheet structure. The β-sheet hydrogen bonding demands at least the presence of a peptide bond (two amino acids). Accordingly, a β-sheet CD profile was observed in the case of the dipeptide incorporated

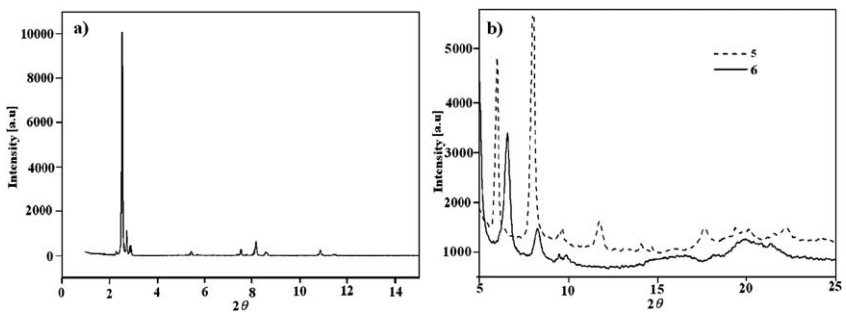

Fig. 5 XRD of the dried gels of (a) **2** and (b) **5** and **6**.

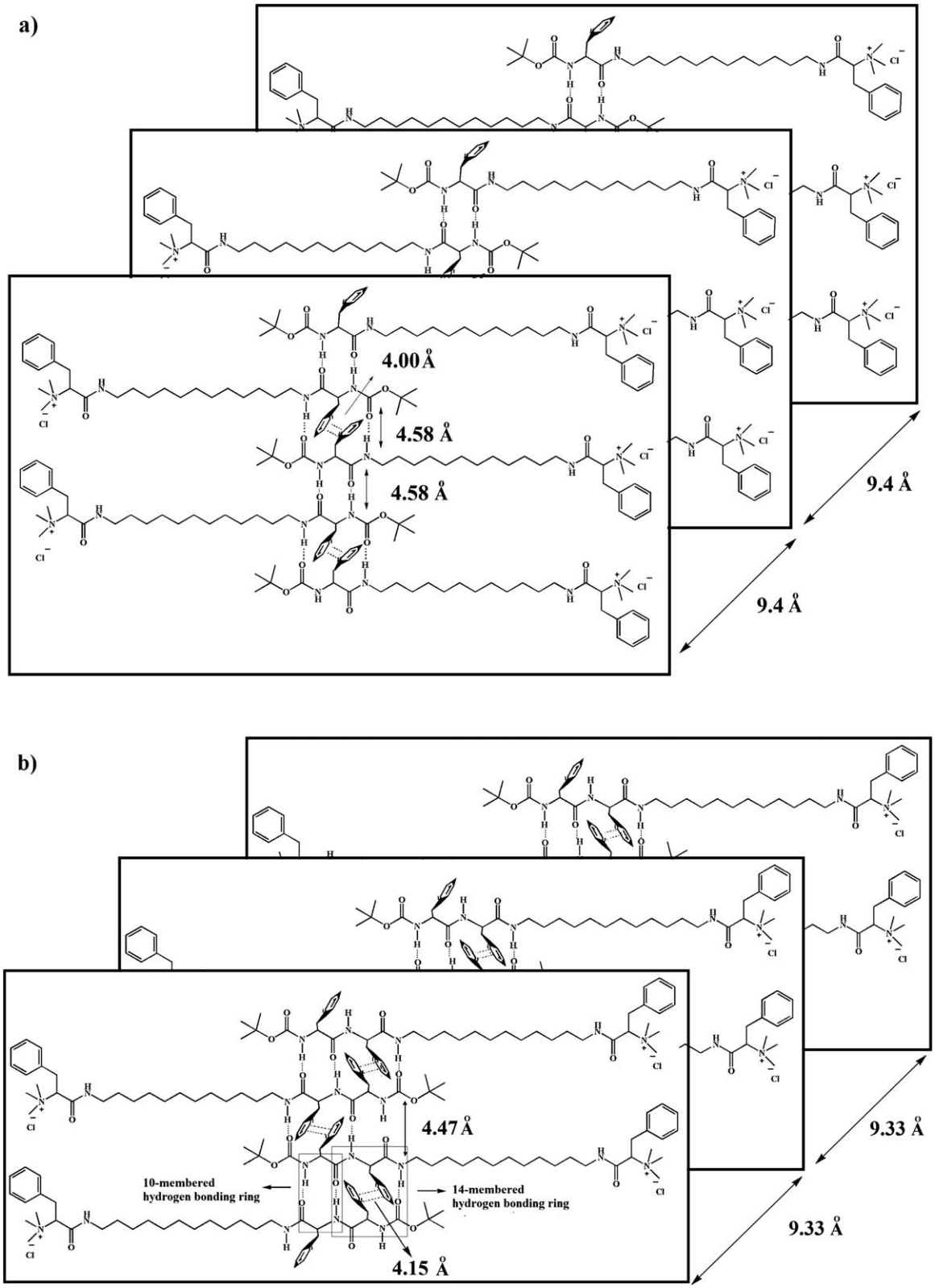

Fig. 6 Probable arrangement of **5** and **6** in the self-assembled gel state.

amphiphile **6**. Furthermore, with increasing monomer concentration there was a sharp increase in peak intensity in both the cases (**5** and **6**). This observation indicates that the formation of supramolecular network originates from the self-assembled organization of individual molecules.[39] The non-covalent packing of the molecules was further confirmed from the temperature dependent CD experiment of **5** and **6** at 0.025%, w/v (Fig. S1, see ESI)† in water. In both the cases, intensity of the CD

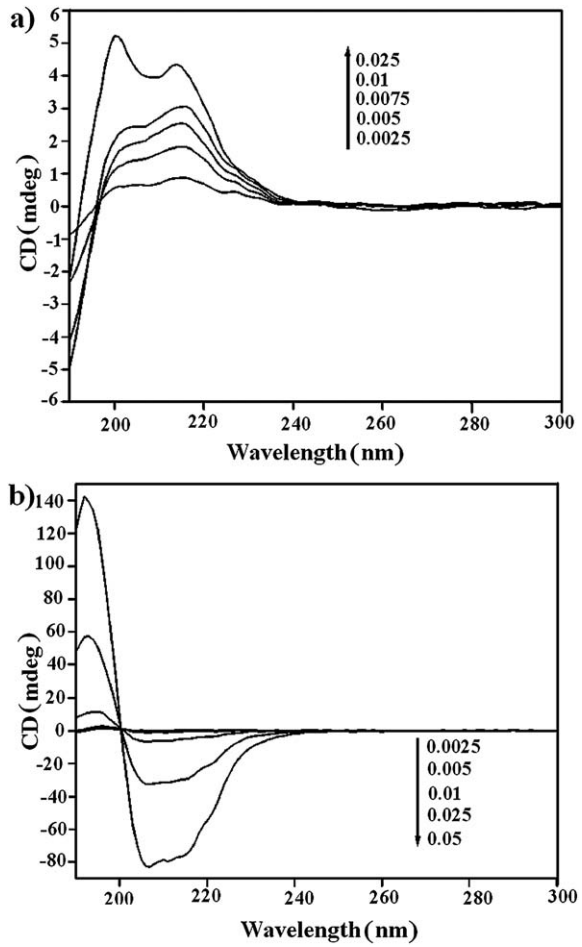

Fig. 7 CD spectra of **5** and **6** with varying concentration (%, w/v) in plain water at 25 °C.

peak gradually decreased with increase in temperature from 20 to 70 °C due to the destruction of the 3D-aggregated structure.

Synthesis of GNP within supramolecular gels

At this point, we were intrigued to exploit these different supramolecular networks obtained through the refinement in the gelator's structure (tail modification) in functional applications like synthesizing gold nanoparticles (GNPs). In this regard, development of soft nanocomposites is rapidly coming up in recent times as advanced functional materials. The low molecular weight gelators with diversified 3D supramolecular orientation (fibers, helices, lamellar, *etc*) have started to gain importance as templates for the synthesis of metal nanoparticles.[50–54] However, it is always desirable if the synthesis and stabilization of GNPs (preferably of specific shape) is achieved at room temperature without the need of any external stabilizing agents.[55–58] Amphiphile **2** has the ability to reduce $HAuCl_4$ to stable spherical shaped GNPs (Fig. S2, ESI).† Interestingly, the presence of extra aromatic amino acid/dipeptide along with amide bond at the tail of the new set of amphiphilic gelators (Fig. 1) with dissimilar self-assembled network compared to **2**, may influence the nanoscale environment which will be offered as the breeding ground for the synthesis of varying shaped GNPs.[51,59–64]

Accordingly we used the present set of amphiphiles for the synthesis of GNPs at their respective MGC. Two different ratios ($HAuCl_4$: gelator concentrations) were used (1 : 10 and 1 : 20), keeping the concentration of the gelator fixed at MGC. All the gelators were capable of synthesizing GNP *in situ* at room temperature without the need of any external reducing agents (see experimental section for details). Formation of GNP was evident from the corresponding surface plasmon resonance (SPR) peak in the UV-vis spectra (Fig. S3, ESI†).[51,59] The shape and size of the *in situ* synthesized GNPs was investigated by taking their TEM images. In the case of gelator **5**, a close view at the TEM image obtained from a 1 : 10 ratio showed the presence of some distinctly octahedral shaped GNPs (Fig. 8a, indicated by arrows and 8b) of 15 to 30 nm dimensions. Also, the corresponding selective area electron diffraction (SAED) pattern revealed the presence of octahedral gold crystals (Fig. 8c). However, in the case of a 1 : 20 concentration ratio of $HAuCl_4$ to gelator (**5**), no such specific shaped GNP was seen in the corresponding TEM image (Fig. 8d). This shape controlled synthesis of GNP in the supramolecular network **5** encouraged us to use the hydrogelators having dipeptides at the alkyl tail (**6** and **8**) at MGC under similar experimental conditions. Interestingly, when chloroaurate ions were reduced by amphiphile **6** (with diphenylalanine at the tail) at a ratio of 1 : 10, the TEM image showed maximum population (~80%) of octahedron shaped GNPs (Fig. 9a–c) with varying sizes of 25 to 45 nm. However, at the concentration ratio of 1 : 20 ($HAuCl_4$: **6**), GNPs of different shapes were formed (2D triangular, decahedron, octahedron and some spherical, Fig. 9d–f). Similarly, in case of **8** at a 1 : 10 ratio, the predominance of octahedron was also unambiguous (Fig. 9g, h), while at a 1 : 20 ratio the shape of nanoparticles was found to

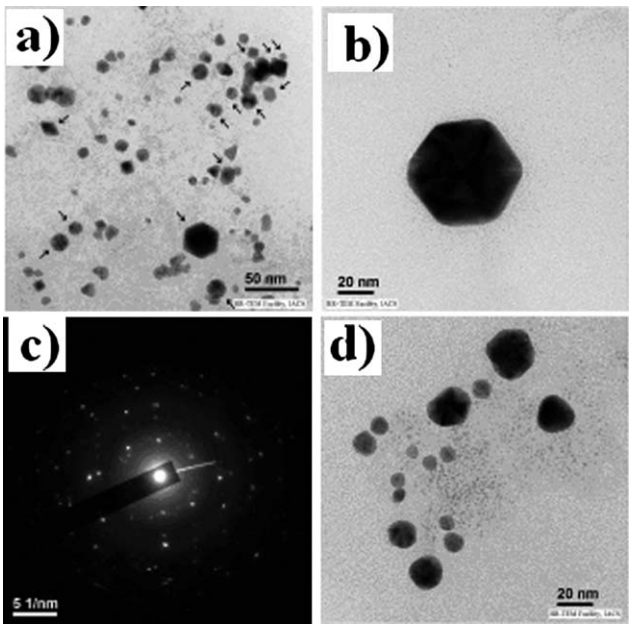

Fig. 8 TEM images of GNPs (a, b in gel **5**) at a 1 : 10 concentration ratio ($HAuCl_4$: **5**) and (c) the corresponding SAED pattern of the synthesized GNP. (d) TEM image of GNPs at 1 : 20 concentration ratio ($HAuCl_4$: **5**). The arrows in (a) indicate octahedral shaped GNPs.

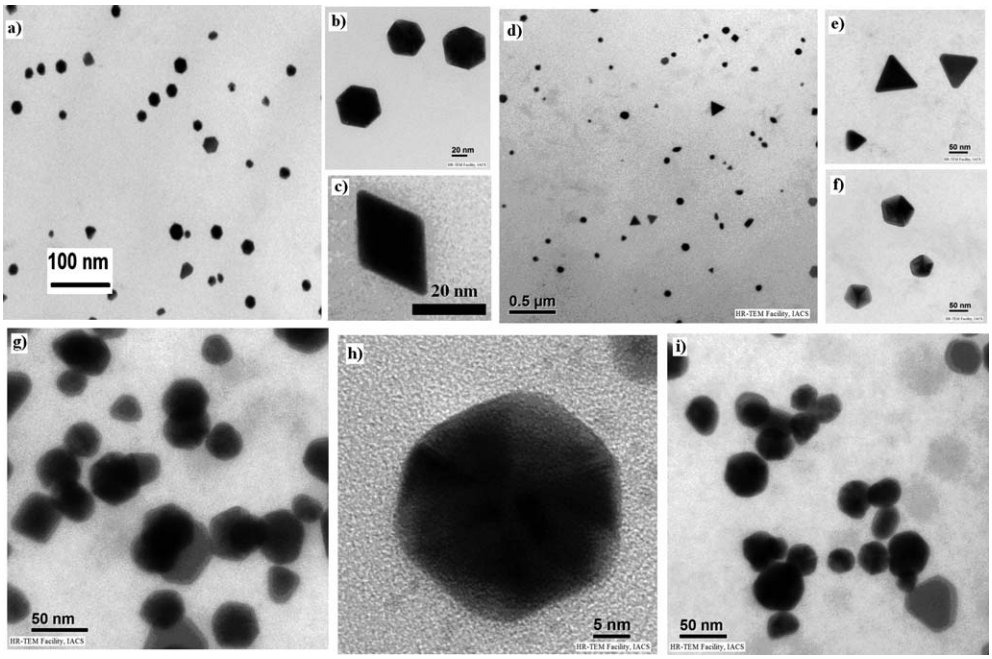

Fig. 9 (a–c) TEM images of GNPs in gel 6 at a 1 : 10 concentration ratio ($HAuCl_4$: **6**) (c shows a tilted octahedron). (d–f) TEM images of GNPs in gel **6** at a 1 : 20 concentration ratio ($HAuCl_4$: **6**) (g and h) TEM image of GNPs in gel **8** at a 1 : 10 concentration ratio ($HAuCl_4$: **8**). (i) TEM image of GNPs in gel **8** at a 1 : 20 concentration ratio ($HAuCl_4$: **8**).

be irregular (Fig. 9i). Hence, the supramolecular nanoscale environment formed due to different mode of self-assembly by the tail modified amphiphilic gelators led to the synthesis of distinctly different shaped GNPs.

Cytocompatibility. Notably, hydrogels have received great attention as potential materials for biological applications; from antibacterial coatings, tissue engineering scaffolds to drug delivery systems and so forth.[55,65–69] In this regard, structural refinements of existing hydrogelators with improved biocompatibility can further bolster these bio-applications. In previous works, it has been proposed that the lipophilic chain of amphiphile can help in the penetration into the cell membrane resulting in cytotoxicity.[70,71] Thus, it is expected that the presence of an amino acid/dipeptide unit at the tail of the amphiphile will presumably diminish the lipophilic content of the alkyl chain and consequently impede the penetration ability of the amphiphile. To this end, the biocompatibility of the tail modified gelators (**5** and **6**) was tested against mammalian cells.[72] Indeed, a significant enhancement of biocompatibility was observed when Boc protected L-phenylalanine/diphenylalanine was tethered to the tail of **1**. The poor cell viability of less than 35% for **1** and **2** (at a concentration of 50 μg/mL, incubated with HepG2 cells for 3 h) enhanced up to ~90% for **5** and **6** (Fig. 10). Even in other concentrations around a 2.5-fold enhancement in the biocompatibility was observed for the gelators **5** and **6** compared to their predecessors with no amino acid at the tail (**1** and **2**). Encouragingly, even at higher concentrations of 200 and 400 μg/mL, the cell viability for both the amphiphiles (**5** and **6**) was always greater than 60%. Hence, the incorporation of *N*-protected amino acid residues at the alkyl tail results in marked improvement in biocompatibility towards mammalian cells.

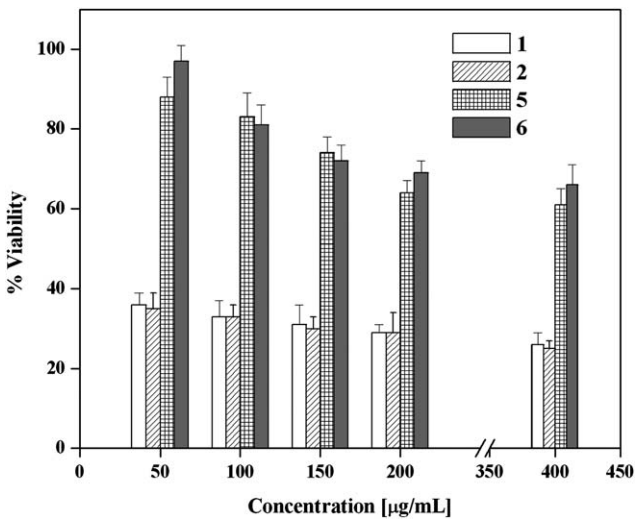

Fig. 10 MTT assay based percent HepG2 cell viability as a function of concentration of **1**, **2**, **5** and **6**. Each percent cell viability point represents the mean ± SD of six determinations.

Experimental section

Materials

All amino acids, di-tert-butyldicarbonate (Boc-anhydride), N, N′-dicyclohexylcarbodiimide (DCC), 1-hydroxybenzotriazole (HOBT), Fmoc chloride, solvents and other reagents were procured from SRL, (India). Trifluoro acetic acid (TFA), iodomethane and sodium hydroxide were purchased from Spectrochem, India. Amberlite Ira 900 chloride ion exchange resins

for ion-exchange, 1,12- diaminododecane, $HAuCl_4$ (30 wt.%) in dilute hydrochloric acid solution, $CDCl_3$ were obtained from Aldrich chemical co. All the materials used in the cell culture study such as DMEM, heat inactivated FBS, trypsin from porcine pancreas and 3-(4,5-dimethyl-2-thiazolyl)-2,5-diphenyl-2H-tetrazolium bromide (MTT) were obtained from Sigma Aldrich Chemical Company. Thin layer chromatography was performed on Merck precoated silica gel 60-F_{254} plates. ^{1}H NMR spectra were recorded in AVANCE 300 MHz (BRUKER) spectrometer. Mass spectrometric data were acquired by the electron spray ionization (ESI) technique on a Q-tof-micro Quadruple mass spectrometer (Micromass).

Synthesis of amphiphiles

A generalized synthetic scheme for all the amphiphiles is given in Scheme S1 (ESI).†

Synthesis of amphiphile 1 and 2

The amphiphiles were synthesized following the reported protocols.[7,19] Briefly, Boc-protected L-phenylalanine was coupled with *n*-dodecylamine (for **1**) and *n*-hexadecylamine (for **2**) using DCC (1 equivalent) and catalytic amount of DMAP in presence of 1 equivalent of HOBT in dry DCM. The product was then purified through column chromatography using 60–120 mesh silica gel and acetone/hexane as the eluent. The obtained amide was then deprotected by trifluoroacetic acid in dry DCM by stirring the reaction for about 2 h. After removing the solvents on a rotary evaporator, the mixture was then taken in ethyl acetate and thoroughly washed with 10% aqueous sodium carbonate solution followed by brine to neutrality. The organic part was then collected over anhydrous Na_2SO_4 and evaporated to dryness to get the primary amine. The primary amine (1 equivalent) thus obtained was quaternized with excess iodomethane using anhydrous potassium carbonate and catalytic amount of 18-crown-6-ether in dry DCM for 2–3 h. The reaction mixture was taken in ethyl acetate and washed with 5% aqueous sodium thiosulphate solution and water. The concentrated ethyl acetate part was then purified through column chromatography using 60–120 mesh silica gel and methanol/chloroform as the eluent. The column-purified material was crystallized from methanol/diethylether to obtain solid quaternized iodide salt. The iodide salt thus obtained was subjected to ion exchange on Amberlite Ira-400 chloride ion exchange resin column followed by crystallization from diethylether to get the pure chlorides (**1**, **2**). Overall yield was 60–70%.

Synthesis of amphiphile 3

In brief, Boc-protected L-phenylalanine was coupled with 1,12-dodecylamine using DCC (2 equivalents) and catalytic amount of DMAP in presence of 2 equivalent of HOBT in dry DCM. The mixture was stirred overnight and the solution was washed with HCl followed by sodium carbonate to isolate the coupled compound. The compound was then column purified using 60–120 mesh silica gel and acetone/hexane as the eluent. The obtained compound was then deprotected using TFA as described above. The diamine III (Scheme S1, ESI)† was then reacted with excess iodomethane using anhydrous potassium carbonate and catalytic amount of 18-crown-6-ether in dry DCM for 2–3 h. The reaction mixture was taken in ethyl acetate and washed with 5% aqueous sodium thiosulphate solution and water. The concentrated ethyl acetate part was then purified through column chromatography using 60–120 mesh silica gel and methanol/chloroform as the eluent. The column-purified material was crystallized from methanol/diethylether to obtain solid quaternized iodide salt. The iodide salt thus obtained was subjected to ion exchange on Amberlite Ira-400 chloride ion exchange resin column followed by crystallization from diethylether to get the pure chlorides (**3**). Overall yield was 60–70%.

Synthesis of amphiphiles 4, 5

Fmoc Chloride (0.8 equivalent) and Boc anhydride (0.8 equivalent) respectively were added drop wise into a solution of diamine III (1 equivalent) in DCM (Scheme S1, ESI).† The solutions were stirred overnight and the mixture was washed with brine to remove the unreacted diamines. The mono protected amines were then isolated and purified through column chromatography using 60–120 mesh silica gel and methanol/chloroform as the eluent. The amine (1 equivalent) thus obtained was quaternized with excess iodomethane using anhydrous potassium carbonate and catalytic amount of 18-crown-6-ether in dry DCM for 2–3 h. The reaction mixture was taken in ethyl acetate and washed with 5% aqueous sodium thiosulphate solution and water. The concentrated ethyl acetate part was then purified through column chromatography using 60–120 mesh silica gel and methanol/chloroform as the eluent. The column-purified material was crystallized from methanol/diethylether to obtain solid quaternized iodide salt. The iodide salt thus obtained was subjected to ion exchange on Amberlite Ira-400 chloride ion exchange resin column followed by crystallization from diethylether to get the pure chlorides (**4**, **5**). Overall yield was 40–50%.

Synthesis of amphiphiles 6–8

The Boc-protected amino acids (L-phenylalanine/L-tryptophan/L-alanine) were selectively coupled with the diamine compound (III) in a similar way (Scheme S1, ESI)† as described above in case of **3**. The Boc-protected amino acid (0.8 equivalent) in dry DCM was added drop wise into a dry DCM solution of the compound III (1 equivalent), HOBt (1.1 equivalent) DCC (1.1 equivalent) and DMAP (1.1 equivalent) under ice cold condition. The reaction was stirred for 12 h at room temperature and usual base work-up was done to remove the unreacted materials. The mono Boc-protected amine was then isolated through column chromatography using 60–120 mesh silica gel and methanol/chloroform as the eluent. Finally the amine was quaternized with excess iodomethane using anhydrous potassium carbonate and catalytic amount of 18-crown-6-ether in dry DCM for 2–3 h. The reaction mixture was taken in ethyl acetate and washed with 5% aqueous sodium thiosulphate solution and water. The concentrated ethyl acetate part was then again purified through column chromatography using 60–120 mesh silica gel and methanol/chloroform as the eluent. The iodide salt thus obtained was subjected to ion exchange on Amberlite Ira-400 chloride ion exchange resin column followed by crystallization from diethylether to get the pure chlorides (**6–8**). Overall yield was 30–35%.

Characterization data for all the amphiphiles are given below except for **2** which was reported earlier.[7] ^{1}H NMR, mass spectra of all other amphiphiles and ^{13}C NMR of most of the gelators are provided in the ESI (Fig. S4–S10).†

Data for 1. Anal calcd (%) for $C_{24}H_{43}N_2OCl$: C, 70.12; H, 10.54; N, 6.81. Found: C, 70.02; H, 10.41; N, 6.76; ^{1}H NMR (300 MHz, $CDCl_3$, 25 °C, TMS) δ = 0.81 (t, 3H, -$(CH_2)_{11}$–CH_3), 1.08–1.23 (br, 20H, –$CH_2(CH_2)_{10}CH_3$), 2.81–3.11 (m, 2H, $CHCH_2Ph$), 3.16–3.19 (d, 2H, $NHCH_2(CH_2)_{10}$), 3.39 (s, 9H, $N(CH_3)_3$), 5.71–5.81 (q, 1H, $COCHNMe_3$), 7.16– 7.29 (m, 5H, aromatic protons), 8.74 (s, 1H, $CONHCH_2$); ESI-MS: *m*/*z*: calcd for $C_{24}H_{43}N_2O$: (the 4° ammonium ion, 100%): 375.3370, found 375.3374 (M^+).

Data for 3. Anal calcd (%) for $C_{36}H_{60}N_4O_2Cl_2$: C, 66.34; H, 9.28; N, 8.60. Found: C, 66.41; H, 9.31; N, 8.53; ^{1}H NMR (300 MHz, $CDCl_3$, 25 °C, TMS): δ = 0.88–1.25 (m, 20H, $CH_2(CH_2)_{10}CH_2$), 2.98–3.08 (m, 4H, $CHCH_2Ph$), 3.23–3.25 (d, 4H, $NHCH_2(CH_2)_{10}CH_2$), 3.68 (s, 18H, $N(CH_3)_3$), 5.59 (t, 2H, $COCHNMe_3$), 7.26–7.32 (m, 10H, aromatic protons), 8.71 (s, 2H, $CONHCH_2$); ESI-MS: *m*/*z*: calcd for $C_{36}H_{60}N_4O_2$: (the 4° ammonium ion, 100%): 580.4705, found 290.2354 (M^+)/2.

Data for 4. Anal calcd (%) for $C_{48}H_{63}N_4O_4Cl$: C, 72.47; H, 7.98; N, 7.04. Found: C, 72.39; H, 8.01; N, 7.13; ^{1}H NMR (300 MHz, $CDCl_3$, 25 °C, TMS): δ = 0.83–1.26 (m, 20H, $CH_2(CH_2)_{10}CH_2$), 2.88–3.20 (m, 8H, CH_2Ph, $NHCH_2(CH_2)_{10}CH_2$), 3.37 (s, 9H, $N(CH_3)_3$), 4.15(t, 1H, COCHNH), 4.28–4.38 (m, 3H, OCH_2CH), 5.57 (s, 1H, $CONHCH_2$), 5.84 (t, 1H, $COCHNMe_3$), 6.14 (s, 1H, OCONHCH), 7.20–7.74 (m, 18H, aromatic protons), 8.77 (s, 1H, $CH_2NHCOCHNMe_3$); ^{13}C NMR (75 MHz, $CDCl_3$): δ 170.84, 164.97, 143.79, 141.32, 136.83, 129.72, 129.44, 128.98, 127.79, 126.99, 73.77, 67.05, 52.82, 47.15, 39.65, 39.57, 39.11, 32.85, 29.42, 29.32, 28.60, 26.66; ESI-MS: *m*/*z*: calcd for $C_{48}H_{63}N_4O_4$: (the 4° ammonium ion, 100%): 759.4844, found 759.4849 (M^+).

Data for 5. Anal calcd (%) for $C_{38}H_{61}N_4O_4Cl$: C, 67.78; H, 9.13; N, 8.32. Found: C, 67.69; H, 9.01; N, 8.23; ^{1}H NMR (300 MHz, $CDCl_3$, 25 °C, TMS): δ = 1.16–1.25 (m, 20H, $CH_2(CH_2)_{10}CH_2$), 1.39 (s, 9H, $OC(CH_3)_3$), 2.93–3.24 (m, 8H, CH_2Ph, $NHCH_2(CH_2)_{10}CH_2$), 3.49 (s, 9H, $N(CH_3)_3$), 4.29 (t, 1H, COCHNH), 5.13 (t, 1H, $COCHNMe_3$), 5.97 (s, 1H, $CONHCH_2$), 6.03 (s, 1H, OCONHCH), 7.20–7.37 (m, 10H, aromatic protons), 8.90 (s, 1H, $CH_2NHCOCHNMe_3$); ^{13}C NMR (75 MHz, $CDCl_3$): δ 164.87, 155.34, 136.93, 129.55, 129.26, 128.74, 79.74, 73.71, 55.84, 52.49, 39.39, 32.65, 29.39, 29.34, 29.12, 28.99, 28.48, 28.19, 26.72, 26.52; ESI-MS: *m*/*z*: calcd for $C_{38}H_{61}N_4O_4$: (the 4° ammonium ion, 100%): 637.4687, found 637.4602 (M^+).

Data for 6. Anal calcd (%) for $C_{47}H_{70}N_5O_5Cl$: C, 68.80; H, 8.60; N, 8.54. Found: C, 68.69; H, 8.65; N, 8.53; ^{1}H NMR (300 MHz, $CDCl_3$, 25 °C, TMS): δ = 1.01–1.25 (m, 20H, $CH_2(CH_2)_{10}CH_2$), 1.31 (s, 9H, $OC(CH_3)_3$), 2.87–3.24 (m, 10H, CH_2Ph, $NHCH_2(CH_2)_{10}CH_2$), 3.46(s, 9H, $N(CH_3)_3$), 4.24 (t, 1H, $NHCHCONHCH_2$), 4.60 (t, 1H, OCONHCHCO), 4.82 (t, 1H, $COCHNMe_3$), 5.76 (s, 1H, $CONHCH_2$), 6.20 (s, 1H, NHCHCONHCHCO), 6.48 (s,1H, OCONHCH), 7.05–7.33 (m, 15H, aromatic protons), 8.68 (s,1H, $CH_2NHCOCHNMe_3$); ^{13}C NMR (75 MHz, $CDCl_3$): δ 170.94, 170.17, 164.90, 162.33, 136.21, 129.64, 129.34, 129.25, 128.98, 128.75, 128.58, 127.79, 127.14, 126.96, 118.16, 80.54, 76.63, 73.52, 52.80, 39.65, 37.84, 32.88, 29.41, 29.34, 29.24, 29.16, 28.15, 26.77. ESI-MS: *m*/*z*: calcd for $C_{47}H_{70}N_5O_5$: (the 4° ammonium ion, 100%): 784.5371, found 784.5347 (M^+).

Data for 7. Anal calcd (%) for $C_{49}H_{71}N_6O_5Cl$: C, 68.47; H, 8.33; N, 9.78. Found: C, 68.49; H, 8.21; N, 9.83; ^{1}H NMR (300 MHz, $CDCl_3$, 25 °C, TMS): δ = 0.90–1.22 (m, 16H, $CH_2(CH_2)_8CH_2$), 1.30 (s, 9H, $OC(CH_3)_3$), 1.38–1.58 (m, 4H, $CH_2(CH_2)_8CH_2$), 3.03–3.24 (m, 8H, CH_2Ph, $NHCH_2(CH_2)_{10}CH_2$), 3.40 (s, 9H, $N(CH_3)_3$), 3.43–3.44 (m, 2H, CH_2-indole), 4.29–4.30 (m, 1H, $NHCHCH_2Ph$), 4.58–4.59 (m, 1H, OCONHCH-Trp), 5.07 (t, 1H, $COCHNMe_3$), 6.40 (s, 1H, NHCHCONHCHCO), 6.85 (s, 1H, OCONHCH), 7.05 (s, 2H, $CONHCH_2$, $CH_2NHCOCHNMe_3$), 7.11–7.34 (m, 15H, aromatic protons), 8.74 (s, 1H, CHNHC); ^{13}C NMR (75 MHz, $CDCl_3$): δ 171.63, 170.41, 164.77, 142.44, 136.40, 133.12, 129.46, 129.27, 128.59, 128.32, 128.23, 127.34, 126.54, 123.60, 121.47, 118.87, 118.40, 111.54, 79.78, 73.57, 69.72, 52.24, 39.86, 39.58, 39.30, 39.19, 39.02, 32.57, 32.48, 29.25, 29.09, 29.00, 28.85, 28.36, 26.61, 26.40. ESI-MS: *m*/*z*: calcd for $C_{49}H_{71}N_6O_5$: (the 4° ammonium ion, 100%): 823.5480, found 823.5471 (M^+).

Data for 8. Anal calcd (%) for $C_{41}H_{66}N_5O_5Cl$: C, 66.15; H, 8.94; N, 9.41. Found: C, 66.10; H, 8.91; N, 9.33; ^{1}H NMR (300 MHz, $CDCl_3$, 25 °C, TMS): δ = 0.98–1.32 (m, 20H, $CH_2(CH_2)_{10}CH_2$), 1.37 (s, 9H, $OC(CH_3)_3$), 1.51–1.62 (m, 3H, $CHCH_3$), 3.03–3.23 (m, 8H, CH_2Ph, $NHCH_2(CH_2)_{10}CH_2$), 3.41 (s, 9H, $N(CH_3)_3$), 4.03–4.04 (d, 1H, $NHCHCH_2Ph$), 4.68 (t, 1H, OCONHCH-Ala), 5.61 (t, 1H, $COCHNMe_3$), 7.04 (s, 2H, $CONHCH_2$, NHCHCONHCHCO), 7.19–7.32 (m, 10H, aromatic protons), 8.43 (s, 2H, OCONHCH, $CH_2NHCOCHNMe_3$); ESI-MS: *m*/*z*: calcd for $C_{41}H_{66}N_5O_5$: (the 4° ammonium ion, 100%): 708.5058, found 708.5048 (M^+).

Preparation of hydrogels

The required amount of the amphiphiles was added in 1 mL water in a screw-capped vial with an internal diameter (i.d.) of 10 mm and slowly heated until the solid was completely dissolved. The solutions were cooled to room temperature without any disturbance. The formation of gel was confirmed by stable to inversion of the glass vial. Gelation study was checked up to 8% w/v.

Microscopic studies

FESEM was performed on a JEOL-6700F microscope. A piece of hydrogel was mounted on glass slide and dried for few hours under vacuum before imaging. The morphology of the dried gels was studied using atomic force microscopy (Veeco, modelAP0100) in non contact mode. A piece of gel was mounted on a silicon wafer and dried for a few hours under vacuum before imaging. TEM measurements were performed on JEOL JEM 2010 microscope. 4 μL of diluted particle suspension in water was

placed on 300-mesh Cu coated TEM grid and dried under vacuum for 4h before taking the TEM images.

FTIR measurements

FTIR measurements of the gelators **2**, **4–6** in $CHCl_3$ solution and in gel state in D_2O were carried out in a Perkin Elmer Spectrum 100 FT-IR spectrometer using KBr and CaF_2 windows, respectively with 1 mm teflon spacers at their MGC.

X-ray diffraction (XRD)

XRD measurements were taken in Seifert XRD 3000P diffractometer and the source was Cu-Kα radiation ($\alpha = 0.15406$ nm) with a voltage and current of 40 kV and 30 mA, respectively. Gel of **2**, **5**, **6** was mounted on the glass slide and dried under vacuum. The xerogels were scanned from 1–40°.

Circular dichroism (CD)

CD spectra of the aqueous solutions of compound **5**, **6** at varying concentration were recorded by using a quartz cuvette of 1 mm path length in a Jasco J-815 spectropolarimeter. Varying temperature CD spectra were also recorded for those compounds at concentration 0.025%, w/v from 20 to 70 °C.

Preparation of GNPs within the hydrogel

The required amount of gelators (50, 7.5, 24 and 19 mg of compound **2**, **5**, **6** and **8** respectively) were taken in 1 mL water and then slowly heated to make a homogeneous solution. Then this solution was cooled at room temperature to form the gel. To this gel, $HAuCl_4$ solution was added very slowly for 5–10 min at room temperature under slow magnetic stirring. The molar concentration ratio of gelator and $HAuCl_4$ was maintained at both 10 : 1 and 20 : 1. Molar concentration of $HAuCl_4$ in gel **2**, **5**, **6**, **8** was at 10.5, 1.1, 2.9, 2.6 mM respectively when gelator : $HAuCl_4$ was at 10 : 1. In the case of a 20 : 1 ratio of gelator to $HAuCl_4$, the concentration of $HAuCl_4$ was accordingly decreased maintaining constant the gelator concentration. The pH of the final reaction mixture was adjusted to 9–10 with a standard 1 N NaOH solution. Gradually the yellow colored $HAuCl_4$ solution became colorless (Au^{+3} to Au^{+1}) and turned to ruby red (Au^{+1} to Au^0) indicating the formation of GNPs. In all cases, 48–72 h was needed for complete conversion.

Cell cultures

Human hepatic cancer derivedHepG2 cells were obtained from the National Center for Cell Science (NCCS), Pune (India), and maintained in DMEM medium supplemented with 10% FBS, 100 mg/L streptomycin and 100 IU/mL penicillin. Cells were grown in a 25 mL cell culture flask and incubated at 37 °C in a humidified atmosphere of 5% CO2 to approximately 70–80% confluence. A subculture was performed every 2–3 days. After 48–72 h, the medium was removed to eliminate the dead cells. Next, the adherent cells were detached from the surface of the culture flask by trypsinization. Cells were now in the exponential phase of growth for checking the viability of the cationic amphiphilic amphiphiles (**1**, **2**, **5**, **6**).

Cytotoxicity MTT assay

The biocompatibility of the amphiphiles was done by microculture MTT reduction assay as reported.[72] This assay is the result from the reduction of a soluble tetrazolium salt by mitochondrial dehydrogenase of the viable tumor cells to an insoluble colored formazan product. The amount of formazan product produced can be spectrophotometrically calculated after dissolution of the dye in DMSO. The enzyme activity and the amount of the formazan produced is proportional to the number of alive cells. The decrease in absorbance value can be attributed to the killing of the cells or inhibition of the cell proliferation by the amphiphiles. HepG2 cells were seeded at a density of 20 000 cells per well in a 96-well microtiter plate for 18–24 h before the evaluation. Concentrated stock solutions (5 mg/mL) of the amphiphiles were sequentially diluted during the experiment to vary the concentrations of the amphiphiles (50–400 μg/mL) in the microtiter plate. The HepG2 cells were incubated with amphiphile **1**, **2**, **5** and **6** for 3 h at 37 °C under 5% CO_2. Then, 10 μL MTT stock solution (5 mg/mL) in phosphate buffer saline was added to the above mixture and the cells were further incubated for another 4 h. The precipitated formazan was dissolved thoroughly in DMSO and absorbance at 570 nm was measured using BioTek® Elisa Reader. The number of surviving cells were expressed as percent viability = (A_{570}(treated cells) − background/A_{570}(untreated cells) − background) × 100.

Conclusion

In summary, the present work finds a rational synthetic approach to significantly augment the gelation ability of existing gelators where a hydrogen bonding moiety like amino acid/dipeptide was judiciously tethered to the tail of an amphiphile. The structure-property relationship was sketched out by investigating a library of tail modified gelators. Spectroscopic and microscopic investigations indicated the formation of anti-parallel hydrogen bonding which eventually forms β-sheet in case of the amphiphile having dipeptide at the tail. The developed gelators had improved functions which can find potential applications in the widely different fields, from material science to biomedicine. Furthermore, the altered self assembly route adopted by the structurally refined amphiphiles results in the conversion of a non-gelator to an excellent gelator which in principle takes us closer to the goal of rational designing of efficient gelators with improved applications.

Acknowledgements

P.K.D. is thankful to the Department of Science and Technology, India for financial assistance. D.D., S.M. and S.B. acknowledge the Council of Scientific and Industrial Research, India for their Research Fellowships. We are thankful to Dr Sisir Debnath for valuable help.

References

1 L. A. Estroff and A. D. Hamilton, *Chem. Rev.*, 2004, **104**, 1201.
2 J. C. Tiller, *Angew. Chem., Int. Ed.*, 2003, **42**, 3072.
3 S. R. Jadhav, P. K. Vemula, R. Kumar, S. R. Raghavan and G. John, *Angew. Chem., Int. Ed.*, 2010, **49**, 7695.

4 S. R. Jadhav, B. S. Chiou, D. F. Wood, G. D. Hoffman, G. M. Glenn and G. John, *Soft Matter*, 2011, **7**, 864.
5 P. Terech, C. Aymonier, A. Loppinet-Serani, S. Bhat, S. Banerjee, R. Das, U. Maitra, A. Del Guerzo and J.-P. Desvergne, *J. Phys. Chem. B*, 2010, **114**, 11409.
6 A. Herres, C. van der Pol, M. Stuart, A. Friggeri, B. L. Feringa and J. van Esch, *J. Am. Chem. Soc.*, 2003, **125**, 14252.
7 A. Shome, S. Debnath and P. K. Das, *Langmuir*, 2008, **24**, 4280.
8 A. M. Bieser and J. C. Tiller, *Chem. Commun.*, 2005, 3942.
9 K. J. C. van Bommel, C. van der Pol, I. Muizebelt, A. Friggeri, A. Heeres, A. Meetsma, B. L. Feringa and J. van Esch, *Angew. Chem., Int. Ed.*, 2004, **43**, 1663.
10 L. A. Estroff and A. D. Hamilton, *Angew. Chem., Int. Ed.*, 2000, **39**, 3447.
11 G. John and P. K. Vemula, *Soft Matter*, 2006, **2**, 909.
12 T. Kar, S. Debnath, D. Das, A. Shome and P. K. Das, *Langmuir*, 2009, **25**, 8639.
13 Z. Yang and B. Xu, *Chem. Commun.*, 2004, 2424.
14 K. Kohler, G. Forster, A. Hauser, B. Dobner, U. F. Heiser, F. Ziethe, W. Richter, F. Steiniger, M. Drechsler, H. Stettin and A. Blume, *Angew. Chem., Int. Ed.*, 2004, **43**, 245.
15 A. M. Bieser and J. C. Tiller, *J. Phys. Chem. B*, 2007, **111**, 13180.
16 F. Fages, F. Vögtle and M. Žinic, *Top. Curr. Chem.*, 2005, **256**, 77.
17 V. Caplar, M. Zinic, J.-L. Pozzo, F. Fages, G. M. Gundert and F. Vögtle, *Eur. J. Org. Chem.*, 2004, 4048.
18 S. Roy, A. Dasgupta and P. K. Das, *Langmuir*, 2007, **23**, 11769.
19 D. Das, A. Dasgupta, S. Roy, R. N. Mitra, S. Debnath and P. K. Das, *Chem.–Eur. J.*, 2006, **12**, 5068.
20 R. N. Mitra, D. Das, S. Roy and P. K. Das, *J. Phys. Chem. B*, 2007, **111**, 14107.
21 S. Debnath, A. Shome, S. Dutta and P. K. Das, *Chem.–Eur. J.*, 2008, **14**, 6828.
22 E. Carretti, M. Bonini, L. Dei, B. H. Berrie, L. V. Angelova, P. Baglioni and R. G. Weiss, *Acc. Chem. Res.*, 2010, **43**, 751.
23 V. A. Mallia, M. George, D. L. Blair and R. G. Weiss, *Langmuir*, 2009, **25**, 8615.
24 S. K. Samanta, A. Pal and S. Bhattacharya, *Langmuir*, 2009, **25**, 8567.
25 S. Dutta, D. Das, A. Dasgupta and P. K. Das, *Chem.–Eur. J.*, 2010, **16**, 1493.
26 N. Mohmeyer, D. Kuang, P. Wang, H.-W. Schmidt, S. M. Zakeeruddin and M. Grätzel, *J. Mater. Chem.*, 2006, **16**, 2978.
27 M. Suzuki, M. Nanbu, M. Yumoto, H. Shiraib and K. Hanabusa, *New J. Chem.*, 2005, **29**, 1439.
28 M. Suzuki, T. Sato, H. Shiraib and K. Hanabusa, *New J. Chem.*, 2006, **30**, 1184.
29 V. Jayawarna, M. Ali, T. A. Jowitt, A. E. Miller, A. Saiani, J. E. Gough and R. V. Ulijn, *Adv. Mater.*, 2006, **18**, 611.
30 R. V. Ulijn and D. N. Woolfson, *Chem. Soc. Rev.*, 2010, **39**, 3349.
31 A. Ajayaghosh and V. K. Praveen, *Acc. Chem. Res.*, 2007, **40**, 644.
32 A. R. Hirst, S. Roy, M. Arora, A. K. Das, N. Hodson, P. Murray, S. Marshall, N. David, J. Sefcik, J. Boekhoven, J. H. Van Esch, S. Santa Barbara, N. T. Hunt and R. V. Ulijn, *Nat. Chem.*, 2010, **2**, 1089.
33 A. R. Hirst, I. A. Coates, T. R. Boucheteau, J. F. Miravet, B. Escuder, V. Castelletto, I. W. Hamley and D. K. Smith, *J. Am. Chem. Soc.*, 2008, **130**, 9113.
34 J. Kyte and R. F. Doolittle, *J. Mol. Biol.*, 1982, **157**, 105.
35 S. Debnath, A. Shome, D. Das and P. K. Das, *J. Phys. Chem. B*, 2010, **114**, 4407.
36 Y. Matsuzawa, K. Ueki, M. Yoshida, N. Tamaoki, T. Nakamura, H. Sakai and M. Abe, *Adv. Funct. Mater.*, 2007, **17**, 1507.
37 H. Rapaport, K. Kjaer, T. R. Jensen, L. Leiserowitz and D. A. Tirrell, *J. Am. Chem. Soc.*, 2000, **122**, 12523.
38 H. Rapaport, H. Grisaru and T. Silberstein, *Adv. Funct. Mater.*, 2008, **18**, 2889.
39 J. H. Jung, S. Shinkai and T. Shimizu, *Chem.–Eur. J.*, 2002, **8**, 2684.
40 J. J. Balbach, Y. Ishii, O. N. Antzutkin, R. D. Leapman, N. W. Rizzo, F. Dyda, J. Reed and R. Tycko, *Biochemistry*, 2000, **39**, 13748.
41 S. J. George and A. Ajayaghosh, *Chem.–Eur. J.*, 2005, **11**, 3217.
42 Nonappa, M. Lahtinen, B. Behera, E. Kolehmainen and U. Maitra, *Soft Matter*, 2010, **6**, 1748.
43 S. Bhattacharya and S. K. Samanta, *Langmuir*, 2009, **25**, 8378.
44 A. Friggeri, C. V. D. Pol, K. J. C. V. Bommel, A. Heeres, M. C. A. Stuart, B. L. Feringa and J. vanEsch, *Chem.–Eur. J.*, 2005, **11**, 5353.
45 Z.-X. Lu, K.-F. Fok, B. W. Erickson and T. E. Hugli, *J. Biol. Chem.*, 1984, **11**, 7368.
46 B. Gratzer, G. M. Holzwarth and P. Doty, *Proc. Natl. Acad. Sci. U. S. A.*, 1961, **47**, 1785.
47 K. H. Mayo, E. Ilyina and H. Park, *Protein Sci.*, 1996, **5**, 1301.
48 I. Laczko, E. Vass, K. Soos, L. Fulop, M. Zarandi and B. Penke, *J. Pept. Sci.*, 2008, **14**, 731.
49 B. Escuder and J. F. Miravet, *Langmuir*, 2006, **22**, 7793.
50 R. N. Mitra and P. K. Das, *J. Phys. Chem. C*, 2008, **112**, 8159.
51 P. K. Vemula and G. John, *Acc. Chem. Res.*, 2008, **41**, 769.
52 S. K. Samanta, A. Pal, S. Bhattacharya and C. N. R. Rao, *J. Mater. Chem.*, 2010, **20**, 6881.
53 S. Dutta, A. Shome, S. Debnath and P. K. Das, *Soft Matter*, 2009, **5**, 1607.
54 A. Shome, S. Dutta, S. Maiti and P. K. Das, *Soft Matter*, 2011, **7**, 3011.
55 N. M. Sangeetha, S. Bhat, G. Raffy, C. Belin, A. Loppinet-Serani, C. Aymonier, P. Terech, U. Maitra, J. P. Desvergne and A. D. Guerzo, *Chem. Mater.*, 2009, **21**, 3424.
56 S. Bhattacharya, A. Srivastava and A. Pal, *Angew. Chem., Int. Ed.*, 2006, **45**, 2934.
57 A. Pal, A. Srivastava and S. Bhattacharya, *Chem.–Eur. J.*, 2009, **15**, 9169.
58 N. M. Sangeetha and U. Maitra, *Chem. Soc. Rev.*, 2005, **34**, 821.
59 T. Kar, S. Dutta and P. K. Das, *Soft Matter*, 2010, **6**, 4777.
60 M. Aslam, L. Fu, M. Su, K. Vijayamohanan and V. P. Dravid, *J. Mater. Chem.*, 2004, **14**, 1795.
61 S. Banerjee, R. K. Das and U. Maitra, *J. Mater. Chem.*, 2009, **19**, 6649.
62 S. K. Das, A. R. Das and A. K. Guha, *Small*, 2010, **6**, 1012.
63 M. H. Rashid and T. K. Mandal, *Adv. Funct. Mater.*, 2008, **18**, 2261.
64 C. J. Murphy, *Science*, 2002, **298**, 2139.
65 D. A. Salick, D. J. Pochan and J. P. Schneider, *Adv. Mater.*, 2009, **21**, 4120.
66 D. A. Salick, J. K. Kretsinger, D. J. Pochan and J. P. Schneider, *J. Am. Chem. Soc.*, 2007, **129**, 14793.
67 S. J. Todd, D. Farrar, J. E. Gough and R. V. Ulijn, *Soft Matter*, 2007, **3**, 547.
68 M. Zelzer and R. V. Ulijn, *Chem. Soc. Rev.*, 2010, **39**, 3351.
69 J. P. Schneider, D. J. Pochan, B. Ozbas, K. Rajagopal, L. Pakstis and J. Kretsinger, *J. Am. Chem. Soc.*, 2002, **124**, 15030.
70 N. Vlachya, D. Tourauda, J. Heilmannb and W. Kunz, *Colloids Surf., B*, 2009, **70**, 278.
71 C. Pantani, N. Spreti, M. C. Maggitti and R. Germani, *Bull. Environ. Contam. Toxicol.*, 2005, **55**, 179.
72 M. B. Hansen, S. E. Nielsen and K. Berg, *J. Immunol. Methods*, 1989, **119**, 203.